Biofilm 4 (2022) 100085

Contents lists available at ScienceDirect

Biofilm

journal homepage: www.sciencedirect.com/journal/biofilm

Exposure of multidrug-resistant *Klebsiella pneumoniae* biofilms to 1,8-cineole leads to bacterial cell death and biomass disruption

Nicolas M. Vazquez [a,b,c], Silvia Moreno [a,c,**], Estela M. Galván [b,c,*]

[a] Laboratorio de Farmacología de Bioactivos Vegetales, Departamento de Investigaciones Bioquímicas y Farmacéuticas, Centro de Estudios Biomédicos, Biotecnológicos, Ambientales y Diagnóstico (CEBBAD), Universidad Maimónides, Buenos Aires, Argentina
[b] Laboratorio de Patogénesis Bacteriana, Departamento de Investigaciones Bioquímicas y Farmacéuticas, Centro de Estudios Biomédicos, Biotecnológicos, Ambientales y Diagnóstico (CEBBAD), Universidad Maimónides, Buenos Aires, Argentina
[c] Consejo Nacional de Investigaciones Científicas y Técnicas (CONICET), Argentina

ARTICLE INFO

Keywords:
Antibiofilm
Klebsiella pneumoniae
Extended-spectrum beta-lactamase
1,8-Cineole
Cell death
Biofilm disruption

ABSTRACT

Klebsiella pneumoniae is a common cause of health-care associated infections. The rise of antibiotic resistance and the ability to form biofilm among *K. pneumoniae* strains are two key factors associated with antibiotic treatment failure. The present study investigates the antibiofilm activity of 1,8-cineole against preformed biofilms of multidrug-resistant extended-spectrum β-lactamase-producing *K. pneumoniae* clinical isolates. To evaluate the antibiofilm activity, cellular viability was analyzed by colony-forming units counting and live/dead staining. In addition, biofilm biomass was evaluated by crystal violet and the biofilm matrix was stained with calcofluor white and observed by confocal laser scanning microscopy. A time- and concentration-dependent effect of the phytochemical over biofilm cell viability was observed revealing that 1% (v/v) 1,8-cineole during 1 h was the optimal treatment condition displaying a significant reduction of cell viability in the preformed biofilms (2.5–5.3 log cfu/cm^2). Furthermore, confocal laser scanning microscopy after SYTO-9 and propidium iodide staining showed that 1,8-cineole was capable of killing bacteria throughout all layers of the biofilm. The compound also caused a biofilm disruption (30–62% biomass reduction determined by crystal violet staining) and a significant decrease in biofilm matrix density. Altogether, our results demonstrate that 1,8-cineole is a promising candidate as a novel antibiofilm agent against multidrug-resistant *K. pneumoniae* strains producing extended-spectrum β-lactamases, given its capability to disrupt the structure and to kill cells within the biofilm.

1. Introduction

Biofilm-producing multidrug-resistant bacteria represent a major health issue worldwide since the infections they cause are associated with high rates of morbidity and mortality [1]. *Klebsiella pneumoniae* is an opportunistic Gram-negative bacterium that causes a variety of antimicrobial-resistant infectious diseases, including urinary tract infections, bacteremia, pneumonia, soft tissue infections, liver abscesses, endophthalmitis and meningitis [2,3].

K. pneumoniae success in causing infections may be partially attributed to its ability to form biofilms. Biofilms are complex bacterial communities surrounded by an extracellular matrix composed of exopolysaccharides, proteins and nucleic acids [4]. Bacteria living in biofilms are known to be difficult to eradicate due to a greater tolerance to antibiotics and host immune defenses when compared to planktonic cells [5]. Another challenge for the eradication of *K. pneumoniae* infections is the increasing incidence of isolates producing carbapenemases and extended-spectrum β-lactamases (ESBLs), enzymes that confer resistance to most β-lactam antibiotics [6].

The World Health Organization classified *K. pneumoniae* as a critical priority for new drug development [7]. Hence, it is very important to screen antibiofilm molecules that can effectively minimize and eradicate infections associated with multidrug-resistant ESBL-producing *K. pneumoniae* with the capability to develop biofilm [8].

Natural products such as plant volatile oils have been studied as a promising alternative to address the diminishing antibiotic pipeline [9].

* Corresponding author. Laboratorio de Patogénesis Bacteriana, Departamento de Investigaciones Bioquímicas y Farmacéuticas, Centro de Estudios Biomédicos, Biotecnológicos, Ambientales y Diagnóstico (CEBBAD), Universidad Maimónides, Buenos Aires, Argentina.
** Corresponding author. Laboratorio de Farmacología de Bioactivos Vegetales, Departamento de Investigaciones Bioquímicas y Farmacéuticas, Centro de Estudios Biomédicos, Biotecnológicos, Ambientales y Diagnóstico (CEBBAD), Universidad Maimónides, Buenos Aires, Argentina.
E-mail addresses: moreno.silvia@maimonides.edu (S. Moreno), galvan.estela@maimonides.edu (E.M. Galván).

https://doi.org/10.1016/j.bioflm.2022.100085
Received 11 July 2022; Received in revised form 29 September 2022; Accepted 3 October 2022
Available online 4 October 2022

The antibacterial activity of these mixtures derived from aromatic and medicinal plants, such as rosemary (*Rosmarinus officinalis*), peppermint (*Mentha piperita*), thyme (*Thymus vulgaris*) and fennel (*Foeniculum vulgare*), have been extensively reported [10]. However, the antimicrobial and antibiofilm activities of isolated compounds from plant oils have not been deeply characterised yet [11].

The phytochemical 1,8-cineole, also known as eucalyptol, can be found in various volatile oils such as eucalyptus oil and rosemary oil and is reported to have antimicrobial, anti-inflammatory, and antioxidant activities [12]. 1,8-Cineole (1,3,3-trimethyl-2-ocxabicyclo [2.2.2]octane) is a bicyclic monoterpene that belongs to the class of organic compounds known as oxanes (compounds containing a six-member saturated aliphatic heterocycle with one oxygen atom and five carbon atoms) (Fig. 1). In a previous study, we reported that 1,8-cineole is one of the main constituents of rosemary essential oil exhibiting antibacterial activity against planktonic cells of enterobacteria such as *K. pneumoniae* and *Escherichia coli* [13]. The bactericidal activity of this compound was associated with a cell membrane permeabilisation effect [13,14]. Similar results were recently found against carbapenemase-producing *K. pneumoniae* isolates [15]. In addition, cell death and biomass reduction in biofilms of MDR ESBL–producing *E. coli* isolates after treatment with 1,8-cineole were reported [16]. Nevertheless, little is known about the antibiofilm activity of 1,8-cineole against MDR ESBL-producing *K. pneumoniae* biofilms.

In this study, we analyzed the effect of 1,8-cineole over cell viability and the biofilm matrix of preformed biofilms of MDR ESBL-producing *K. pneumoniae* clinical isolates.

2. Materials and methods

2.1. Bacterial isolates and inoculum preparation

Klebsiella pneumoniae strains used in this study were isolated from adult patients and are described in Table 1. Strains named Kp AM were isolated from urinary samples collected from patients admitted to a medical center at Buenos Aires City (Argentina) between 2017 and 2018 [18]. Strains Kp010 and Kp05 were isolated from patients with catheter-associated urinary tract infections, Pirovano Hospital (Buenos Aires City, Argentina) [14,17]. Microbiological susceptibility testing was carried out by standard methods based on CLSI breakpoints [19]. *K. pneumoniae* isolates were examined for ESBL production by a double-disk synergy test using ceftazidime, cefotaxime and cefepime with and without clavulanic acid according to CLSI guidelines [19]. *K. pneumoniae* clinical strains used in this study were isolated as part of routine clinical hospital procedures to diagnose infection and hence ethical approval was not required, according to the corresponding institutional guidelines.

Isolates were maintained in the laboratory as frozen stocks (at −80 °C) in Luria-Bertani (LB) broth supplemented with 15% glycerol. Inocula for assays were prepared as described previously [16]. Briefly, isolates were streaked on Tryptic Soy Broth (TSB)-agar plates and grown overnight at 37 °C. Subsequently, individual colonies were used to inoculate TSB (2 ml) and were incubated overnight at 37 °C and 200 rpm. Then, each inoculum was properly diluted in M9 minimal medium supplemented with 0.8% glucose in order to obtain 10^7 cells/ml.

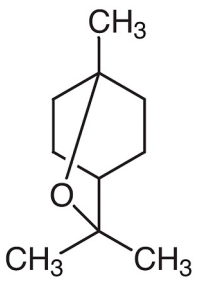

Fig. 1. Chemical structure of 1,8-cineole.

Table 1
K. pneumoniae isolates used in this study.

Strain	Antibiotic resistance[a]	Source
Kp010	AMP	[14]
KpAM1S	AMP	This work
KpAM4S	AMP	This work
KpAM4	AMK, AMC, AMP, CAZ, CEF, CIP, CTX, NIT, GEN, TMS, TZP	This work
KpAM7	AMC, AMP, CAZ, CEF, CIP, CTX, NIT, TMS	This work
Kp05	AMP, CHL, CAZ, CEF, CTX, GEN, NAL, RIF, TET	[17]

[a] AMK, amikacin; AMC, amoxicillin-clavulanic acid; AMP, ampicillin; CHL, chloramphenicol; CAZ, ceftazidime; CEF, cephaloridine; CIP, ciprofloxacin; CTX, cefotaxime; NIT, Nitrofurantoin; GEN, gentamicin; NAL, nalidixic acid; RIF, rifampicin; TMS, trimethoprim sulfamethoxazole; TET, tetracycline; TZP, piperacillin/tazobactam.

2.2. Biofilm formation assays

Bacterial inocula in M9 supplemented with 0.8% glucose (1×10^7 cells/ml) were placed in 96-well (200 μl per well) or 24-well (1 ml per well) polystyrene plates (DeltaLab, Barcelona, Spain) and incubated statically at 37 °C. Biofilms were developed in M9 given that this minimal medium was reported to support a more robust biofilm formation by Enterobacteria, such as *E. coli* and *K. pneumoniae*, than a reach medium (for example, LB) [14,20]. Adhesion to polystyrene surface was allowed for 3 h and then the medium was replaced every 24 h for up to 2 d. At selected time points, biofilms developed in 96-well plates were washed three-times with sterile 0.9% NaCl before biomass quantification by crystal violet staining (absorbance measurement at 595 nm) [21]. All crystal violet assays were performed in technical triplicates and, for each plate, three wells were used as blanks containing sterile growth medium. Biofilm biomass levels were classified as highly positive ($A_{595} \geq 1$), low-grade positive ($0.2 \leq A_{595} \leq 1$), or negative ($A_{595} \leq 0.2$) [22].

For quantification of cultivable cells, biofilms developed in 24-well plates were washed with sterile 0.9% NaCl before mechanical disruption from the surface as previously described [23]. The bacterial suspensions obtained were serially 10-fold diluted, plated on TSB-agar plates, and grown for 16 h at 37 °C for enumeration of colony forming units (cfu). Experiments were done in biological triplicates and technical duplicates were performed.

2.3. Biofilm susceptibility to 1,8-cineole

As already described, 1,8-cineole (Sigma, MO, USA) (0.25–2%, v/v) in M9 supplemented with 0.8% glucose and 0.5% Tween 80 were prepared from an 80% (v/v) pure compound solution in ethanol [16]. Preformed biofilms (2 d) were washed with 0.9% NaCl, then, the indicated concentration of 1,8-cineole was carefully added on top of the biofilms, and the plates were incubated statically at 37 °C. Untreated controls were carried out by replacing the culture medium by fresh medium. Vehicle controls were assessed using ethanol concentrations corresponding to each phytochemical dilution used in medium supplemented with 0.5% Tween 80 (ethanol concentrations of 0.03, 0.06, 0.12, 0.25, 0.50%, v/v, corresponding to 1,8-cineole concentrations of 0.12, 0.25, 0.50, 1.00, 2.00%, v/v, respectively). After 15–180 min of incubation, the medium was removed, biofilms washed with 0.9% NaCl and biofilm biomass and cell viability were determined as explained before. Experiments were done in biological triplicates and technical duplicates were performed.

2.4. Biofilm imaging

KpAM7 and Kp05 biofilms were formed on 12-mm glass coverslips,

as described previously [16]. Preformed biofilms (2 d) were treated with 1% (v/v) 1,8-cineole during 1 h. Controls were carried out as explained above. Bacterial viability in biofilms was assayed using the live/dead BacLight™ Bacterial Viability Kit (Thermo Fisher Scientific, Waltham, MA, USA) containing SYTO®9 green-fluorescent nucleic acid stain and the red-fluorescent nucleic acid stain, propidium iodide, which was handled following the provider's recommendations. Biofilm matrix was analyzed by calcofluor-white (Sigma, MO, USA) staining. All staining procedures were carried out at room temperature in the dark for 30 min, with the following final concentrations: SYTO®9 (5 μM), propidium iodide (30 μM), calcofluor-white (0.5 mM). Observation of biofilms was done using a Nikon Eclipse T1 confocal laser scanning microscope (CLSM) (Nikon Corporation, Tokyo, Japan). Representative images (frames of 123 × 123 μm) were taken with an image resolution of 512 × 512 pixels. For each biofilm, six image-stacks were taken at different locations throughout the biofilm, using 1-μm z-step increments. Unstained and single-stained slices for each dye were used to monitor and subtract all respective background signals. COMSTAT 2.1 (www.comstat.dk) [24,25] and the ImageJ software [26] were utilised to quantify the viable (SYTO®9; green), dead (propidium iodide; red), colocalized (SYTO®9 + propidium iodide; yellow) cells. Colocalized fluorescence was defined as part of propidium iodide staining, as the dye was able to penetrate the membrane. As it did not completely remove SYTO®9, it was subtracted from SYTO®9 staining. Orthogonal and 3D reconstructions images for cell viability assays were generated by Icy software [27], while Huygens Essential software (Scientific Volumetric Imaging, Netherlands) was used to obtain biofilm matrix (calcofluor--white, cyan) z-stack maximum intensity projections (MIP) and 3D reconstructions images.

2.5. Statistical analysis

Statistical significance between control and 1,8-cineole-treated samples was determined with either paired Student's t-test (one-tailed) or the one-way analysis of variance (ANOVA) followed by Bonferroni post-hoc test, using GraphPad Prism software version 9 (GraphPad Software, San Diego, CA, USA). Differences were considered significant when P values were less than 0.05.

3. Results

3.1. Biofilm-forming capability of K. pneumoniae isolates

The capability to produce biofilm of six *K. pneumoniae* clinical isolates was studied over time (1–2 d) for three MDR ESBL-producing strains (KpAM4, KpAM7 and Kp05) and three antibiotic-sensitive isolates (Kp010, KpAM1S and KpAM4S) by crystal violet staining (Fig. 2). By day two, all isolates showed large amounts of biofilm biomass production (A_{595nm} between 1.04 and 3.71), being at least twice the amount of biomass observed at 1 d. All isolates were categorized as highly-positive biofilm producers after 2 d, with Kp05 and KpAM7 producing the highest (A_{595nm} 3.71 ± 0.18) and the lowest (A_{595nm} 1.04 ± 0.22) biofilm biomass, respectively. These two MDR ESBL-producing strains were chosen for further experiments.

3.2. Defining conditions for optimal 1,8-cineole antibiofilm treatment by viable cell counting

Optimal 1,8-cineole antibiofilm treatment conditions were determined for the selected strains: Kp05 and KpAM7. First, increasing phytochemical concentrations (0.125–2%, v/v) were added onto 2-*d*-old biofilms and after incubation during 1 h, viable cell counts were determined (Fig. 3A). The corresponding amount of vehicle control (ethanol: 0.03–0.5%, v/v) was also tested. Fig. 3A shows that 1,8-cineole had a concentration-dependent detrimental effect on biofilm cell viability in both Kp05 and KpAM7, while the vehicle (ethanol) did not show any

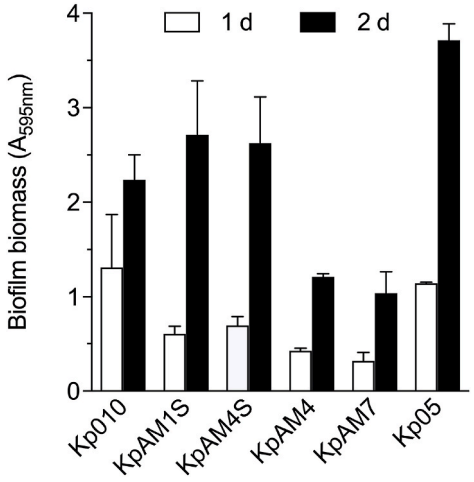

Fig. 2. Biofilm formation of *K. pneumoniae* clinical isolates. Biofilms were developed in M9 medium onto polystyrene plates and biofilm biomass was determined by crystal violet staining (A_{595nm}) after one and two days. Values are means of at least two biological replicates, and error bars indicate standard error.

effect at all. Significant decrease in biofilm cell viability was observed at a phytochemical concentration of 0.5–2% (v/v), diminishing the cfu by approximately 5.0-log in Kp05 and 2.5-log in KpAM7. At lower 1,8-cineole concentrations no effect over viability was observed in any of the two isolates.

Fig. 3B shows a time-dependent reduction in biofilm cell viability in both isolates using 1% (v/v) of the phytochemical. After 1 h treatment, 5.3-log and 2.5-log decrease for Kp05 and KpAM7, respectively, was observed. A slight increase in the number of viable cells was detected for Kp05 after 3 h of treatment.

In summary, optimal 1,8-cineole antibiofilm treatment conditions were defined as the challenge of a pre-formed biofilm with 1% (v/v) 1,8-cineole for 1 h.

3.3. Cell viability evaluation in K. pneumoniae biofilms after 1,8-cineole treatment by live/dead staining and confocal microscopy

To further investigate the effect of 1,8-cineole over biofilm cell viability, qualitative and quantitative image-based analyses were carried out by live/dead staining. Live/dead staining is used to evaluate membrane integrity as it employs a red dye that only enters cells with damaged membranes (PI) and a green dye that stains both intact and compromised membranes (SYTO®9) (Fig. 4).

Fig. 4A–B shows the qualitative analysis of live/dead assay, which evidenced a high amount of dead cells stained in red by propidium iodide in both isolates after treatment with 1% (v/v) of 1,8-cineole. By contrast, vehicle-treated controls (0.25% v/v of ethanol) appeared mostly green, indicating that biofilm cells were predominantly alive. In fact, 1,8-cineole treatment produced a total cell death throughout all layers of Kp05 biofilm (Fig. 4A, bottom panels; Supplementary Fig. S1), including cells located at the bottom layers of the biofilm (Fig. 4A, upper panels; Supplementary Fig. S1). On the other hand, the compound was able to kill up to two thirds of the biofilm formed by the KpAM7 isolate, with living cells being observed near substratum (Fig. 4B, upper panels; Supplementary Fig. S2). In biofilms of both isolates, an increase in cell-free zones at the solid surface were visualized after 1,8-cineole treatment in comparison with the vehicle-treated controls (Fig. 4A–B, upper panels).

Quantification of total live/dead cells confirmed the high amount of dead cells after treatment with 1% (v/v) of 1,8-cineole in both KpAM7 and Kp05 biofilms (Fig. 4C). The percentages of dead cells were 99% and 91% for Kp05 and KpAM7, respectively. On the other hand, cells in

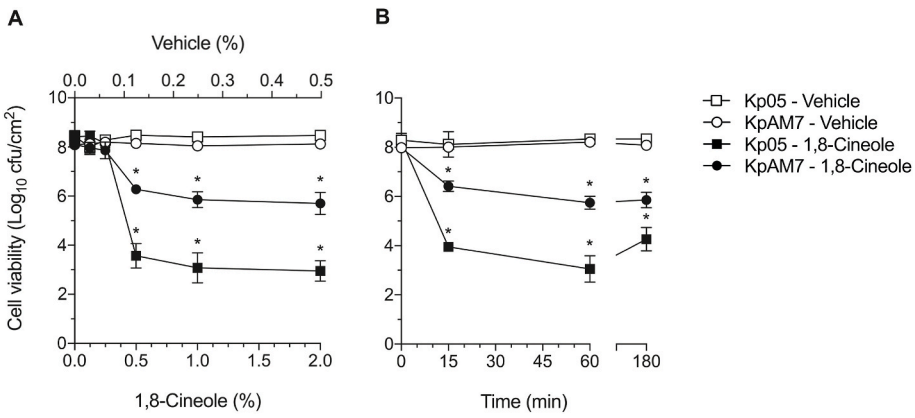

Fig. 3. Concentration-response and time-course effect of 1,8-cineole over cell viability in MDR ESBL-producing *K. pneumoniae* biofilms. Two-day-old biofilms of *K. pneumoniae* isolates KpAM7 and Kp05 were studied and the number of viable cells was assessed as described in the Materials and Methods section. **(A)** Biofilms treated with increasing concentrations of 1,8-cineole and vehicle (ethanol) for 1 h. Values are means of three biological replicates and error bars indicate standard deviations. (*) $p < 0.05$ compared to vehicle-treated biofilms for each strain by one-way ANOVA followed by Bonferroni post-hoc test. **(B)** Time-course effect of 1% (v/v) 1,8-cineole and vehicle (ethanol) on biofilms. Values are means of three biological replicates and error bars indicate standard deviations. (*) $p < 0.05$ compared to vehicle-treated biofilms for each strain by Student's *t*-test.

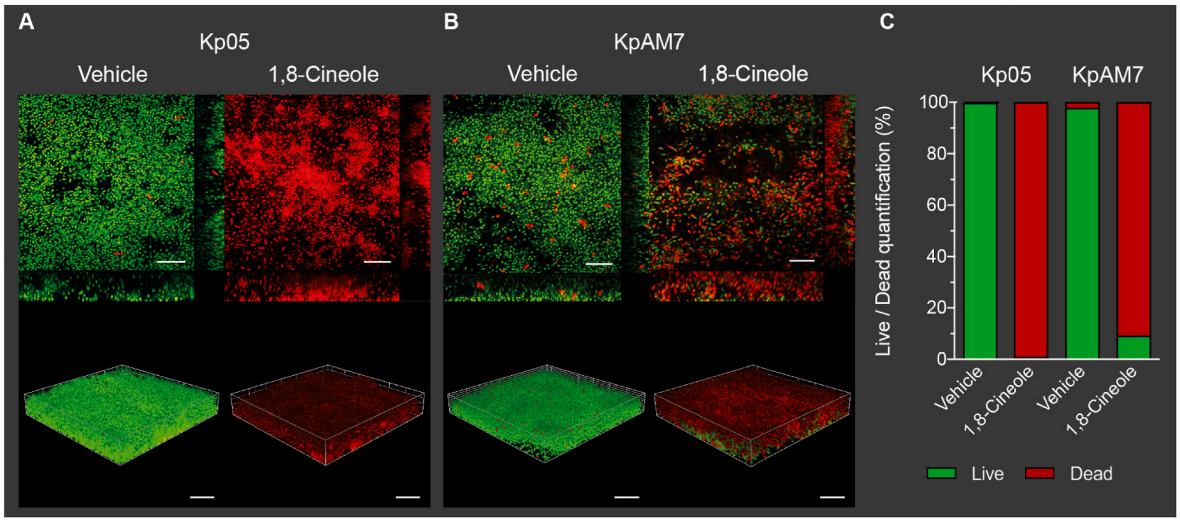

Fig. 4. Confocal laser scanning microscopy of live/dead biofilm cells after 1,8-cineole treatment. Two-day-old biofilms of MDR ESBL-producing strains Kp05 and KpAM7 incubated for 1 h with 1% (v/v) 1,8-cineole or 0.25% ethanol (vehicle), were stained with live/dead BacLight™ Bacterial Viability Kit. Live (green) or dead (red/yellow) bacterial cells were visualized by CLSM and quantified by COMSTAT. Representative images of the bottom layers, taken at 2 μm above the surface **(A-B, upper panels)** and total 3D reconstruction image of the biofilm **(A-B, lower panels)** of the two isolates are shown. Scale bars: 20 μm. **(C)** COMSTAT analysis of biomass. For each of the six z-stacks from two independent biological replicates, the % of live and dead bacteria was calculated. Z-stack galleries can be found in Supplementary Fig. 1S and Fig. 2S. (For interpretation of the references to colour in this figure legend, the reader is referred to the Web version of this article.)

vehicle-treated biofilms remained mostly viable (less than 2% of dead cells).

The results described above, evidence that 1,8-cineole is capable of affecting viability in both upper and deeper layers of the biofilm, even reaching cells at substratum on some occasions.

3.4. *Effect of 1,8-cineole treatment on K. pneumoniae biofilm structural integrity*

Next, we investigated whether the phytochemical, in addition to killing biofilm cells, can alter its structural integrity. First, possible disruption of biofilm biomass after 1 h treatment with 1% (v/v) 1,8-cineole was monitored by crystal violet staining. Fig. 5 shows a significant reduction in the biofilm biomass after phytochemical treatment for both Kp05 and KpAM7 preformed biofilms (62 ± 4 and 30 ± 7% reduction, respectively) in comparison to vehicle-treated controls.

The biofilm matrix has been reported to contribute to the biofilm structure and stability [28]. Hence, we studied whether treatment with 1,8-cineole can cause changes to the biofilm matrix leading to the previously observed biofilm biomass loss.

For this, calcofluor white staining followed by confocal laser scanning microscopy analysis was performed over two-day-old Kp05 and KpAM7 biofilms. Matrix z-stack maximum intensity projections and 3D reconstructions images evidenced a loss of density and disturbance of structural integrity of the biofilm matrix after treatment for 1 h with 1% (v/v) of 1,8-cineole (Fig. 6). A strong reduction in biofilm matrix was observed in Kp05 after treatment in comparison with its vehicle-treated control (Fig. 6A), whereas in KpAM7 changes were subtler (Fig. 6B). Notably, after 1,8-cineole treatment more matrix-free zones throughout all layers of the biofilm were visualized in both isolates in comparison with its vehicle-treated controls (Supplementary Figs. S3–4).

All these findings suggest that 1,8-cineole, besides killing cells all along the biofilm, also disturbs its structural integrity causing a significant decrease in biofilm matrix density and biomass.

4. Discussion

MDR biofilm-producing *K. pneumoniae* strains are generally associated with chronicity of infections and high tolerance to antibiotic treatments in a variety of clinical settings [3]. There are currently very few effective treatments to combat MDR *K. pneumoniae* infections. Our findings demonstrate that 1,8-cineole was capable of both a significant

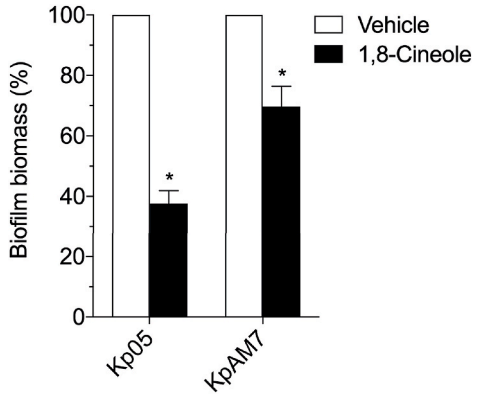

Fig. 5. Effect of 1,8-cineole over *K. pneumoniae* biofilm biomasses. Two-day-old biofilms of Kp05 and KpAM7 isolates were challenged with 1% (v/v) 1,8-cineole or 0.25% ethanol (vehicle) for 1 h, and the remaining biofilm biomass was quantified by crystal violet staining. Biomass production of vehicle-treated controls (A_{595nm} 3906 and 1817 for Kp05 and KpAM7, respectively) corresponds to 100%. Mean values of three biological replicates, and error bars indicate standard deviations. (*) $p < 0.05$ compared to vehicle by Student's *t*-test.

reduction in the number of viable biofilm cells and a concomitant biomass disruption of preformed biofilms of MDR ESBL-producing *K. pneumoniae* clinical isolates. These effects were achieved at a similar concentration of the compound (1% v/v) that was effective against planktonic MDR and non-MDR *E. coli* and *K. pneumoniae* strains [13,14]. Interestingly, we have also demonstrated in this study that a high anti-biofilm efficacy against MDR ESBL-producing *K. pneumoniae* strains was reached after a very short exposure to 1,8-cineole (1 h).

According to CLSM results obtained after SYTO-9 and propidium iodide staining, 1,8-cineole treatment killed cells at both upper and deeper layers of *K. pneumoniae* biofilms. This result suggests that 1,8-cineole has a good penetration into the biofilm causing cell death in the whole structure. It has been postulated that small non-polar constituents of plant volatile oils could have a high biofilm penetration potential because they have a superior diffusion coefficient compared to common antibiotics [29]. We found a similar effect of 1,8-cineole against MDR ESBL-producing *E. coli*, where the compound penetrates through the biofilm causing cell death and biomass reduction [16].

As detected by CLSM using propidium iodide as indicator of bacterial viability, the cells within the biofilm were almost entirely red after exposure to 1,8-cineole revealing that the cell membranes were seriously damaged. Therefore, biofilm cell death observed after the phytochemical treatment is probably due to a membrane permeabilisation effect. We have earlier demonstrated a permeabilisation effect of 1,8-cineole on *K. pneumoniae* planktonic cells [14]. Also, it has been recently described a disruption of bacterial cell membrane after 1, 8-cineole treatment of carbapenemase-producing *Klebsiella pneumoniae* [15].

Reports on the inhibitory activity of natural products against biofilm-producing *K. pneumoniae* are limited. Eucalyptus and thyme oils presented strong biofilm inhibitory activity against biofilm-producing isolates including *Klebsiella*, while clove oil showed weak inhibition [30, 31]. In addition, two isolated plant-derived terpenes, eugenol and paeoniflorin, have shown a deteriorating impact on cell viability within carbapenem-resistant *K. pneumoniae* biofilms [32,33]. Recently, the phytochemical diterpenoid phytol evidenced antibiofilm activity against carbapenem-resistant and ESBL-positive *K. pneumoniae*, by inhibiting initial cell attachment and by altering the extracellular matrix architecture [34].

Biofilm matrix architecture is essential for biofilm stability and functionality [28]. In *K. pneumoniae*, this matrix is largely composed of polysaccharides [35] associated to proteins and extracellular DNA [36].

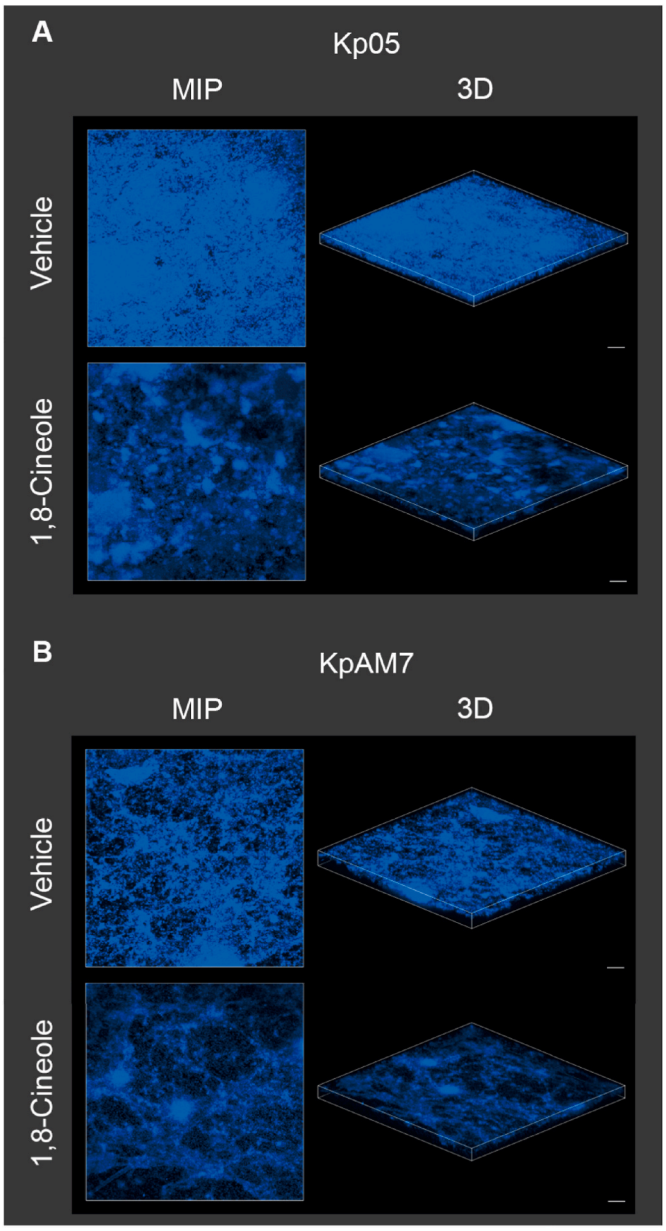

Fig. 6. Calcofluor white-stained *K. pneumoniae* biofilm matrices observed by confocal laser scanning microscopy after treatment with 1,8-cineole. Two-day-old biofilms of Kp05 **(A)** and KpAM7 **(B)** isolates, incubated with 1% (v/v) 1,8-cineole or 0.25% ethanol (vehicle) during 1 h, were stained with calcofluor white (cyan). Z-stack maximum intensity projections of biofilm matrices (MIP, **left panels)** and total 3D reconstruction images of biofilm (3D, **right panels)** are shown. Scale bars: 50 μm. Z-stack galleries can be found in Supplementary Fig. 3S and Fig. 4S. (For interpretation of the references to colour in this figure legend, the reader is referred to the Web version of this article.)

Our CLSM results of calcofluor white staining showed alteration of the biofilm matrix integrity after 1,8-cineole treatment. The literature indicates a knowledge gap in molecular interactions between phytochemicals and matrix components; here we propose alternatives to explain our findings. One possible explanation could be that 1,8-cineole can penetrate the biofilm, even reaching cells in the deeper layers, and then cause disruption of the cell membrane integrity, leading to cell death and releasing of the cellular content in the surroundings. In this sense, it has been reported that terpenoids primarily target the cytoplasmic membrane through the accumulation of hydrophobic phenolic groups in the lipid bilayer. This accumulation could disrupt

lipid–protein interaction, increase membrane permeability, accelerate the leakage of cell contents and ultimately destroy cell integrity [37]. Other authors have reported the ability of terpenes, such as thymol, carvacrol and citral, to disrupt microbial biofilms and showed that terpenes enhanced cell permeability, resulting in pore formation and efflux of the intracellular content [38]. In this context, released hydrolytic enzymes could degrade the biofilm matrix, a fact that would explain the observed loss of matrix density and the biofilm biomass reduction after 1,8-cineole treatment. In this regard, periplasmic glycosidase enzymes capable of cellulose (BcsZ) and poly-β(1,6)-N-acetyl-D-glucosamine (PgaB) disassembly has been reported in *K. pneumoniae* [39,40]. Moreover, incubation of purified *E. coli* PgaB with preformed poly-β(1,6)-N-acetyl-D-glucosamine-dependent biofilms, including *E. coli*, completely disrupted the biofilm within 2 h [41]. Another possible explanation that cannot be ruled out, is that1,8-cineole initiates the disruption of the matrix structure by creating micropores or microchannels to enter into biofilm, which is a mechanism already proposed for phytochemicals with antibiofilm activity [42].

As stated, the present study demonstrates the anti-biofilm activity of 1,8-cineole against preformed *K. pneumoniae* biofilms. Even though it is beyond the scope of this study, further research is needed to address the effect of 1,8-cineole in early stages of biofilm formation, including bacterial adhesion to the substratum surface and initial maturation.

To design an effective novel antibiofilm strategy using1,8-cineole, several aspects should be considered, including phytochemical hydrophobicity, toxicity and active concentration to be applied. Selection among management options may depend on the type of application to be developed, either to treat biofilm-infected tissues or to remove biofilms from medical devices (urinary catheters, prosthetic heart valves, central venous catheters, vascular prosthesis, intravenous catheters and cardiac pacemakers). To overcome the limited aqueous solubility of 1,8-cineole, a range of delivery platforms has been reported, such as emulsions, liposomes, polymer-particles and micelles [43,44]. For biofilms growing on inert surfaces it is feasible to apply the active concentration of the compound reported here (1% v/v). On the other hand, for treating biofilms related to tissue infections, toxicity data is important. To the best of our knowledge, there is little information on the toxicity and cytotoxicity of 1,8-cineole. For instance, cytotoxicity assays performed on tumor-derived cell lines showed an IC50 of 0.11–0.35% v/v [45,46]. *In vivo* toxicity assessment of oral administration of 1,8 cineole in mice revealed a LD50 value of 3.8 g/kg, which suggested a low acute toxic potency of this compound [47]. It is important to note that the active concentration of 1,8-cineole can be reduced by encapsulation and/or combinatorial treatment with antibiotics [48,49]. Further studies are still required regarding formulation and delivery.

In summary, we have demonstrated that 1,8-cineole is capable of entering deep in the biofilm, kill MDR ESBL-producing *K. pneumoniae* cells efficiently, and disrupt the preformed biofilm. Therefore, 1,8-cineole is a potentially useful antibiofilm agent against MDR ESBL-producing Enterobacteriaceae.

CRediT authorship contribution statement

Nicolas M. Vazquez: Conceptualization, Methodology, Formal analysis, Investigation, Writing – original draft, Visualization. **Silvia Moreno:** Conceptualization, Methodology, Validation, Formal analysis, Resources, Writing – review & editing, Project administration, Funding acquisition. **Estela M. Galván:** Conceptualization, Methodology, Validation, Formal analysis, Resources, Writing – review & editing, Project administration, Funding acquisition.

Declaration of competing interest

The authors declare that they have no known competing financial interests or personal relationships that could have appeared to influence the work reported in this paper.

Data availability

Data will be made available on request.

Acknowledgments

We are grateful to Claudia Garbasz, Head of the Microbiology Service at the Hospital General de Agudos “Dr. I. Pirovano” (Buenos Aires city, Argentina) for providing the clinical bacterial isolates. This work was supported by PICT grant number 2017-0183 from Agencia Nacional de Promocion Cientifica y Tecnologica, Argentina, to EMG; and intramural funding from Fundacion Cientifica Felipe Fiorellino, Universidad Maimonides, Argentina, to SM. NMV is a doctoral fellow, SM and EMG are researcher members of CONICET. The authors would like to thank Dr. Carol Davies-Salas for a thorough language revision of the manuscript.

Appendix A. Supplementary data

Supplementary data to this article can be found online at https://doi.org/10.1016/j.bioflm.2022.100085.

References

[1] Song X, Liu P, Liu X, Wang Y, Wei H, Zhang J, Yu L, Yan X, He Z. Dealing with MDR bacteria and biofilm in the post-antibiotic era: application of antimicrobial peptides-based nano-formulation. Mater Sci Eng C 2021;128:112318.
[2] Gonzalez-Ferrer S, Peñaloza HF, Budnick JA, Bain WG, Nordstrom HR, Lee JS, Tyne D Van. Finding order in the chaos: outstanding questions in Klebsiella pneumoniae pathogenesis. Infect Immun 2021;89.
[3] Guerra MES, Destro G, Vieira B, Lima AS, Ferraz LFC, Hakansson AP, Darrieux M, Converso TR. Klebsiella pneumoniae biofilms and their role in disease pathogenesis. Front Cell Infect Microbiol 2022;12.
[4] Donlan RM, Costerton JW. Biofilms: survival mechanisms of clinically relevant microorganisms. Clin Microbiol Rev 2002;15:167–93.
[5] Hall CW, Mah T-F. Molecular mechanisms of biofilm-based antibiotic resistance and tolerance in pathogenic bacteria. FEMS Microbiol Rev 2017;41:276–301.
[6] Karaiskos I, Giamarellou H. Carbapenem-sparing strategies for ESBL producers: when and how. Antibiotics 2020;9:61.
[7] Tacconelli E, et al. Discovery, research, and development of new antibiotics: the WHO priority list of antibiotic-resistant bacteria and tuberculosis. Lancet Infect Dis 2018;18:318–27.
[8] Zhang K, Li X, Yu C, Wang Y. Promising therapeutic strategies against microbial biofilm challenges. Front Cell Infect Microbiol 2020;10.
[9] Aljaafari MN, AlAli AO, Baqais L, Alqubaisy M, AlAli M, Molouki A, Ong-Abdullah J, Abushelaibi A, Lai K-S, Lim S-HE. An overview of the potential therapeutic applications of essential oils. Molecules 2021;26:628.
[10] Tariq S, Wani S, Rasool W, Shafi K, Bhat MA, Prabhakar A, Shalla AH, Rather MA. A comprehensive review of the antibacterial, antifungal and antiviral potential of essential oils and their chemical constituents against drug-resistant microbial pathogens. Microb Pathog 2019;134:103580.
[11] Mulat M, Pandita A, Khan F. Medicinal plant compounds for combating the multi-drug resistant pathogenic bacteria: a review. Curr Pharmaceut Biotechnol 2019;20:183–96.
[12] Brown SK, Garver WS, Orlando RA. 1,8-cineole: an underappreciated anti-inflammatory therapeutic. J Biomol Res Therapeut 2017;6.
[13] Ojeda-Sana AM, van Baren CM, Elechosa MA, Juarez MA, Moreno S. New insights into antibacterial and antioxidant activities of rosemary essential oils and their main components. Food Control 2013;31:189–95.
[14] Moreno S, Galvan EM, Vazquez NM, Fiorilli G, Caceres Guido PA. Antibacterial efficacy of Rosmarinus officinalis phytochemicals against nosocomial multidrug-resistant bacteria grown in planktonic culture and biofilm. In: Mendez-Vilas A, editor. The battle against microbial pathogens: basic science, technological adv. And educational programs; 2015. p. 3–8.
[15] Moo C-L, Osman MA, Yang S-K, Yap W-S, Ismail S, Lim S-H-E, Chong C-M, Lai K-S. Antimicrobial activity and mode of action of 1,8-cineol against carbapenemase-producing Klebsiella pneumoniae. Sci Rep 2021;11:20824.
[16] Vazquez NM, Mariani F, Torres PS, Moreno S, Galván EM. Cell death and biomass reduction in biofilms of multidrug resistant extended spectrum β-lactamase-producing uropathogenic Escherichia coli isolates by 1,8-cineole. PLoS One 2020;15:e0241978.
[17] Galvan EM, Mateyca C, Ielpi L. Role of interspecies interactions in dual-species biofilms developed in vitro by uropathogens isolated from polymicrobial urinary catheter-associated bacteriuria. Biofouling 2016;32:1067–77.
[18] Martinez A. Estudio microbiológico de bacterias Gram negativas multirresistentes en orina y sangre en pacientes internados: producción de biofilm y actividad antibiofilm de fitoquímicos en aislados clínicos de alta prevalencia. (Biochemistry thesis). Buenos Aires: Universidad Maimonides; 2018.
[19] CLSI. Performance standards for antimicrobial susceptibility testing. 29th ed. Clinical and Laboratory Standards Institute; 2018.

[20] Naves P, del Prado G, Huelves L, Gracia M, Ruiz V, Blanco J, Rodríguez-Cerrato V, Ponte MC, Soriano F. Measurement of biofilm formation by clinical isolates of Escherichia coli is method-dependent. J Appl Microbiol 2008;105:585–90.
[21] Ferrières L, Hancock V, Klemm P. Specific selection for virulent urinary tract infectious *Escherichia coli* strains during catheter-associated biofilm formation. FEMS Immunol Med Microbiol 2007;51:212–9.
[22] Lagha R, Ben Abdallah F, Al-Sarhan BO, Al-Sodany Y. Antibacterial and biofilm inhibitory activity of medicinal plant essential oils against Escherichia coli isolated from UTI patients. Molecules 2019;24.
[23] Juarez GE, Galvan EM. Role of nutrient limitation in the competition between uropathogenic strains of Klebsiella pneumoniae and Escherichia coli in mixed biofilms. Biofouling 2018;34:287–98.
[24] Heydorn A, Nielsen AT, Hentzer M, Sternberg C, Givskov M, Ersboll BK, Molin S. Quantification of biofilm structures by the novel computer program COMSTAT. Microbiology 2000;146(Pt 1):2395–407.
[25] Vorregaard M. Comstat2 - a modern 3D image analysis environment for biofilms. In: Informatics and mathematical modelling. Denmark: Tech. Univ. Denmark Kongens Lyngby; 2008.
[26] Schneider CA, Rasband WS, Eliceiri KW. NIH Image to ImageJ: 25 years of image analysis. Nat Methods 2012;9:671–5.
[27] de Chaumont F, et al. Icy: an open bioimage informatics platform for extended reproducible research. Nat Methods 2012;9:690–6.
[28] Flemming H-C, Wingender J, Szewzyk U, Steinberg P, Rice SA, Kjelleberg S. Biofilms: an emergent form of bacterial life. Nat Rev Microbiol 2016;14:563–75.
[29] Nazzaro F, Fratianni F, De Martino L, Coppola R, De Feo V. Effect of essential oils on pathogenic bacteria. Pharmaceuticals 2013;6:1451–74.
[30] Mathur S, Udgire M, Khambhapati A, Paul D. Anti-biofilm activity and bioactive component analysis of eucalyptus oil against urinary tract pathogen. Int J Curr Microbiol Appl Sci 2014;3:912–8.
[31] Radünz M, da Trindade MLM, Camargo TM, Radünz AL, Borges CD, Gandra EA, Helbig E. Antimicrobial and antioxidant activity of unencapsulated and encapsulated clove (Syzygium aromaticum, L.) essential oil. Food Chem 2019;276:180–6.
[32] Qian W, Zhang J, Wang W, Wang T, Liu M, Yang M, Sun Z, Li X, Li Y. Antimicrobial and antibiofilm activities of paeoniflorin against carbapenem-resistant *Klebsiella pneumoniae*. J Appl Microbiol 2020;128:401–13.
[33] Qian W, Sun Z, Wang T, Yang M, Liu M, Zhang J, Li Y. Antimicrobial activity of eugenol against carbapenem-resistant Klebsiella pneumoniae and its effect on biofilms. Microb Pathog 2020;139:103924.
[34] Adeosun IJ, Baloyi IT, Cosa S. Anti-biofilm and associated anti-virulence activities of selected phytochemical compounds against Klebsiella pneumoniae. Plants 2022;11.
[35] Birarda G, Delneri A, Lagatolla C, Parisse P, Cescutti P, Vaccari L, Rizzo R. Multi-technique microscopy investigation on bacterial biofilm matrices: a study on Klebsiella pneumoniae clinical strains. Anal Bioanal Chem 2019;411:7315–25.
[36] Singh AK, Yadav S, Chauhan BS, Nandy N, Singh R, Neogi K, Roy JK, Srikrishna S, Singh RK, Prakash P. Classification of clinical isolates of Klebsiella pneumoniae based on their in vitro biofilm forming capabilities and elucidation of the biofilm matrix chemistry with special reference to the protein content. Front Microbiol 2019;10.
[37] Wu Y, Bai J, Zhong K, Huang Y, Qi H, Jiang Y, Gao H. Antibacterial activity and membrane-disruptive mechanism of 3-p-trans-Coumaroyl-2-hydroxyquinic acid, a novel phenolic compound from pine needles of cedrus deodara, against Staphylococcus aureus. Molecules 2016;21.
[38] Kumari P, Arora N, Chatrath A, Gangwar R, Pruthi V, Poluri KM, Prasad R. Delineating the biofilm inhibition mechanisms of phenolic and aldehydic terpenes against cryptococcus neoformans. ACS Omega 2019;4:17634–48.
[39] Huang T-W, Lam I, Chang H-Y, Tsai S-F, Palsson BO, Charusanti P. Capsule deletion via a λ-Red knockout system perturbs biofilm formation and fimbriae expression in Klebsiella pneumoniae MGH 78578. BMC Res Notes 2014;7:13.
[40] Römling U, Galperin MY. Bacterial cellulose biosynthesis: diversity of operons, subunits, products, and functions. Trends Microbiol 2015;23:545–57.
[41] Little DJ, et al. PgaB orthologues contain a glycoside hydrolase domain that cleaves deacetylated poly-β(1,6)-N-acetylglucosamine and can disrupt bacterial biofilms. PLoS Pathog 2018;14:e1006998.
[42] Uddin Mahamud AGMS, Nahar S, Ashrafudoulla M, Park SH, Ha S-D. Insights into antibiofilm mechanisms of phytochemicals: prospects in the food industry. Crit Rev Food Sci Nutr 2022:1–28.
[43] Makabenta JMV, Nabawy A, Li C-H, Schmidt-Malan S, Patel R, Rotello VM. Nanomaterial-based therapeutics for antibiotic-resistant bacterial infections. Nat Rev Microbiol 2021;19:23–36.
[44] Li C-H, Chen X, Landis RF, Geng Y, Makabenta JM, Lemnios W, Gupta A, Rotello VM. Phytochemical-based nanocomposites for the treatment of bacterial biofilms. ACS Infect Dis 2019;5:1590–6.
[45] Wang W, Li N, Luo M, Zu Y, Efferth T. Antibacterial activity and anticancer activity of rosmarinus officinalis L. Essential oil compared to that of its main components. Molecules 2012;17:2704–13.
[46] Kahkeshani N, Hadjiakhoondi A, Navidpour L, Akbarzadeh T, Safavi M, Karimpour-Razkenari E, Khanavi M. Chemodiversity of Nepeta menthoides Boiss. & Bohse. essential oil from Iran and antimicrobial, acetylcholinesterase inhibitory and cytotoxic properties of 1,8-cineole chemotype. Nat Prod Res 2018;32:2745–8.
[47] Xu J, et al. Acute and subacute toxicity study of 1,8-cineole in mice. Int J Clin Exp Pathol 2014;7:1495–501.
[48] Krogsgård Nielsen C, Kjems J, Mygind T, Snabe T, Schwarz K, Serfert Y, Meyer RL. Antimicrobial effect of emulsion-encapsulated isoeugenol against biofilms of food pathogens and spoilage bacteria. Int J Food Microbiol 2017;242:7–12.
[49] Zacchino SA, Butassi E, Liberto M Di, Raimondi M, Postigo A, Sortino M. Plant phenolics and terpenoids as adjuvants of antibacterial and antifungal drugs. Phytomedicine 2017;37:27–48.